EUROfusion

WPMAT-CPR(17) 17726

F Klein et al.

Oxidation resistance of plasma-facing tungsten alloys

Preprint of Paper to be submitted for publication in Proceeding of 18th International Conference on Fusion Reactor Materials (ICFRM-18)

This work has been carried out within the framework of the EUROfusion Consortium and has received funding from the Euratom research and training programme 2014-2018 under grant agreement No 633053. The views and opinions expressed herein do not necessarily reflect those of the European Commission.

Oxidation Resistance of Plasma-Facing Tungsten Alloys

F. Klein[1], T. Wegener[1], A. Litnovsky[1], M. Rasinski[1], X. Y. Tan[1,2], J. Gonzalez Julian[1], J. Schmitz[1,3], M. Bram[1], J. W. Coenen[1] and Ch. Linsmeier[1]

[1] *Forschungszentrum Jülich GmbH, Institut für Energie- und Klimaforschung, 52425 Jülich, Germany*

[2] *School of Materials Science and Engineering, Hefei University of Technology, Hefei, 23009, China*

[3] *Department of Applied Physics, Ghent University, 9000 Ghent, Belgium*

Abstract

Tungsten (W) currently is the main candidate as plasma-facing armour material for the first wall of future fusion reactors, like DEMO. Advantages of W include a high melting point, a high thermal conductivity, a low tritium retention, and a low erosion yield. However, in case of an accident, air ingress into the vacuum vessel can occur and the temperature of the first wall can reach 1200 K to 1450 K due to nuclear decay heat. In the absence of cooling, the temperature will remain in that range for several weeks. At these temperatures the radioactive tungsten oxide volatilizes. Therefore, 'smart' W alloys are developed. Smart alloys aim at preserving the properties of W during plasma operation coupled with suppressed tungsten oxide formation in case of an accident.

This study focusses on oxidation studies at 1273 K of samples produced by mechanical alloying followed by field assisted sintering. In a first step the sintering is optimized for tungsten (W) - chromium (Cr) -yttrium (Y) alloys. It is shown that the best oxidation resistance is achieved with small grains. A grain size of 0.17 µm is achieved. This yields a closed, protective oxide layer. In a second step the grinding process is analysed. It is shown that scratches initiate failure of the protective oxide. In a third step the oxidation and sublimation is measured for weeks - for the first time the sublimation is explicitly measured. It is shown that the oxidation is suppressed in comparison to pure W. However, sublimation at a rate of 1×10^{-6} mg cm^{-2} s^{-1} starts after a few days. Nevertheless, the progess in smart alloys is evident: sublimation is delayed by about two days and complete mechanical destruction of the first wall is avoided.

Keywords: W-based alloys, W-Cr-Y alloys, oxidation resistance, DEMO

1. Introduction

The future DEMOnstration power plant (DEMO) aims to demonstrate the technological and economical feasibility of fusion as a future energy source. This implies that the power plant must be safe and ecologically friendly. This is very challenging as the plasma facing components will have to withstand an unprecedented fluence of particles, radiation, and neutrons. These conditions make tungsten (W) a prime candidate as plasma facing material. Advantages include a low sputtering yield by plasma ions, a good thermal conductivity, a low tritium retention, and a high melting temperature [1, 2, 3]. Further, the radioactive isotopes which are generated by neutron irradiation decay to shielded hands-on level within 100 years [4].

One important safety criterion is that there should be full passive safety in a Loss-of-Coolant-Accident (LOCA) with simultaneous air ingress. During operation neutrons activate the W, as soon as the cooling system fails it heats up due to its nuclear decay heat. Modelling predicts a temperature rise to 1200 K to 1450 K where it remains for around 100 days [5]. In the presence of air, which may penetrate the vacuum vessel through leaks, the W oxidises rapidly at such temperatures. It forms radioactive WO_3 which then sublimates. Several hundreds of kg week^{-1} sublimate at 1273 K and above [6]. On top of that, the W has a volume ratio of 3.4 [7]. This can cause strong tensions, breaking the W and detaching it from the first wall. In such a state emergency measures are even more difficult.

The aim is to solve these problems by developing a new W alloy. One the one hand it must retain the beneficial properties of W for operation of the power plant. On the other hand it must form a protective layer in case of a loss-off-coolant accident. This protective layer shall full-fill two goals: firstly, the formation of WO_3 must be stopped so that no radioactive W is released to the environment. Secondly, the first wall shall not disassemble in an uncontrolled way and not pose additional challenges to potential emergency measures.

It was shown that alloys containing tungsten (W), 11.4 weight (wt.) % chromium (Cr), and 0.6 wt. % yttrium (Y) are a promising candidate [8, 9, 10]. In the following this is written as W-11.4Cr-0.6Y. The Cr was found to form a protective oxide scale on the surface suppressing the formation of WO_3. The Y was found to be crucial to support the formation of this protective oxide scale. However, these studies were conducted with thin films on the time-scale of a few hours. This study aims at investigating the oxidation and sublimation behaviour of these alloys over several weeks - a time-scale relevant for DEMO. This requires a large material reservoir, bulk samples. They are produced by Field Assisted Sintering Technology (FAST).

In a first step, different FAST parameters are tested to produce the novel W-Cr-Y alloys. In a second step, the influence of the grinding is studied. In a third step, the oxidation and sublimation characteristics for weeks in synthetic air at 1273 K is studied.

2. Experimental

The samples are produced by Field Assisted Sintering Technology (FAST) [11]. Firstly, the W, Cr, and Y powders are mixed and milled in a planetary ball mill, Retsch PM400. After 60 h of milling a homogeneous powder is achieved - more details on the mechanical alloying procedure can be found in ref. [9]. Secondly, the powder is packed in a graphite foil and a graphite die to be sintered in the FAST device FCT-HPD5, FCT Systeme GmbH. Sintering is achieved by applying a pressure (50 MPa), and heating using a current generated by a DC pulse generator. The heating rate is chosen in the range of 100 K min^{-1} to 200 K min^{-1}, the maximum temperature is chosen in the range of 1733 K to 1823 K. The obtained sample is cut using a diamond blade saw and ground using a planar grinding and polishing machine. Grinding removes the first 0.5 mm where carbon from the foil during sintering penetrated and creates a reproducible surface finish. Unless stated differently, the final grinding step is performed using a P1200-grade silicon carbide abrasive paper.

The density of the samples is measured by Archimedes principle. The mass is measured using the Sartorius MSA225P micro-balance having resolution of 10 µg, whereas the volume is determined by the mass of the displaced ethanol using the same micro-balance.

Oxidation is performed in a thermogravimetric analyzer, the TAG-16/18 from Setaram. It allows to measure the in-situ mass change of a sample in a temperature range of 300 K to 2000 K. The drift of the scale for isothermal oxidations with the duration of several days is at 2×10^{-8} mg s^{-1}. This is possible due to a symmetrical, dual furnace design: one furnace contains the sample, the other furnace contains an inert product with the same volume to compensate buoyancy effects. It is possible to measure both, the oxidation rate and the sublimation rate. The oxidation rate is determined by the mass increase of the sample as oxygen is added to the material. The mass increase of the sample is measured by placing the sample into an alumina crucible which is attached to the balance by a platinum wire.

The sublimation rate is measured indirectly as illustrated in Fig. 1: an alumina tube is attached to the balance using a platinum wire. The sample hangs inside the tube attached to a different platinum wire. Thus, there is no direct contact between the sample and the tube at the balance. As soon as sublimation of the sample starts, part of the material will resublimate onto the alumina tube and cause a mass increase which is measured. The present work assumes that all material resublimates onto the alumina tube and that no material re-resublimates from the tube. Thus, the given sublimation rates are a lower boundary.

Further, the combined Scanning Electron Microscopy (SEM) - Focussed Ion Beam (FIB) system Carl Zeiss CrossBeam XB540 equipped with an Energy Dispersive X-ray analysis (EDX) is used. This provides insights into the grain structure and the structure and composition of the oxide layers. Before cutting a cross section, typically a layer of platinum (Pt) is deposited on top to protect the surface structures.

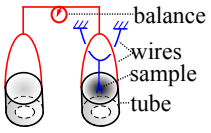

Figure 1: Schematic of the sublimation measurement setup.

The surface roughness is measured using the Dektak 6M from Bruker. A diamond-tipped stylus with a diameter of 2 µm is moved across the sample. The mechanical movement of the stylus yields a 2D-surface profile.

3. Results

3.1. Material optimisation

There are four main methods to produce W-Cr-Y samples: Hot Isostatic Pressing (HIP) [12], pressureless sintering [13], Field Assisted Sintering Technology (FAST), and magnetron sputtering [8, 6]. Magnetron sputtering allows quick production of a large number of samples. One obtains a thin film with a thickness of around 3.5 µm and a homogeneous solution of W, Cr, Y, see Fig. 2 a. The grain size is of around 0.1 µm. Fig. 2 e shows that this alloy forms a protective, closed Cr_2O_3 layer with some internal Cr_2O_3 when exposed to 1273 K at 20 kPa O_2 and 80 kPa Ar partial pressure. This protective oxide layer meets the main requirement - stopping the formation of WO_3.

However, due to the small thickness the material reservoir of thin films is small: bulk samples are required for long studies. This study employs FAST - a key advantage compared to HIP and pressureless sintering is that the sintering happens within minutes and grain growth can be controlled better. The main parameters which can be tuned are the heating rate h, the maximum sintering temperature T_{max}, and the holding time t_{hold}.

The first sample is produced with $h = 200$ K min^{-1}, $T_{\mathrm{max}} = 1823$ K, and $t_{\mathrm{hold}} = 1$ min. A relative density of 98.5 % and large grains with a size of 1 µm is achieved. The oxidation performance is shown in Fig. 3. Frequent breakaway oxidation is found - breakaway oxidation should be understood as a short, temporal increase of the mass gain rate. The oxidation rate is 1000 times slower than of pure W. However, further improvement is desired. Based on the experience with thin films, the following production steps aim at achieving a smaller grain size.

A smaller grain size can be achieved with a lower sintering temperature T_{max} as grain growth happens slower at lower temperatures. Different samples are prepared with fixed $T_{\mathrm{max}} = 1733$ K and the following combinations of the heating rate h and the holding time t_{hold}:

- ($h = 100$ K min^{-1}, $t_{\mathrm{hold}} = 1$ min) yields a relative density of 98 % and large grains with a size of 1.0 µm, see Fig. 2 b.
- ($h = 200$ K min^{-1}, $t_{\mathrm{hold}} = 1$ min) yields a relative density of 99 % and medium grains with a size of 0.25 µm, see Fig. 2 c.
- ($h = 200$ K min^{-1}, $t_{\mathrm{hold}} = 0$ min) yields a relative density of 99 % and small grains with a size of 0.17 µm, see Fig. 2 d.

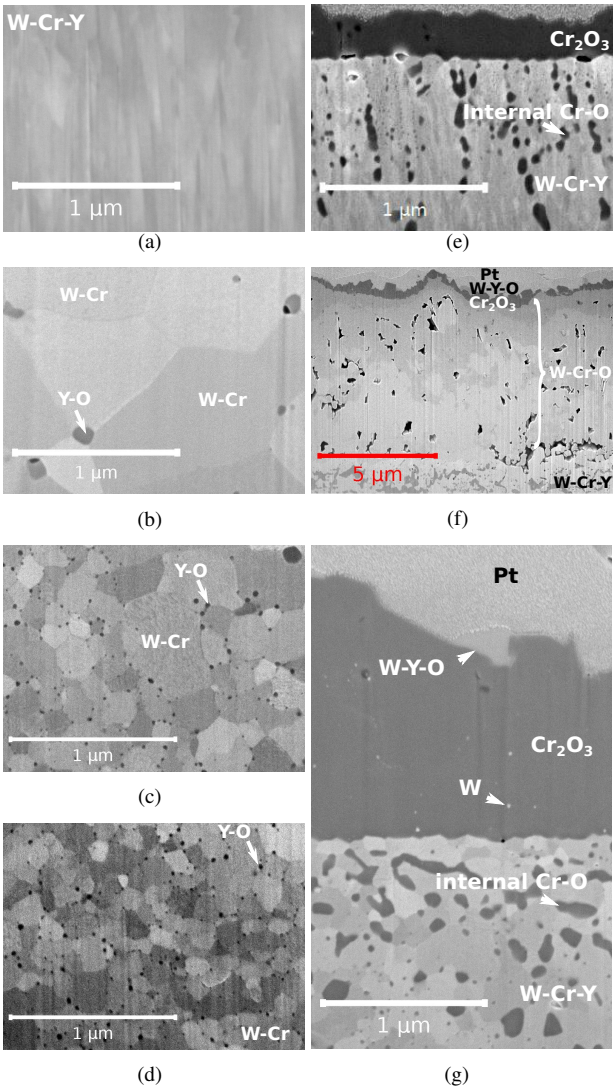

Figure 2: Electron microscopy images of cross sections. (a)-(d) show the microstructure before oxidation. (a) is a thin film prepared by magnetron sputtering. (b)-(d) are bulk samples prepared by FAST with a maximum sintering temperature T_{max} = 1733 K where (b) has large grains, (c) medium grains, and (d) small grains. (e)-(g) show the microstructure after oxidation at a temperature of 1273 K at 20 kPa O_2 and 80 kPa Ar partial pressure. (e) shows sample (a) after 75 min of oxidation. (f) shows sample (b) after 44 h of oxidation. (g) shows sample (d) after 44 h of oxidation.

The mass gain due to oxidation at 1273 K in 20 kPa O_2 and 80 kPa Ar partial pressure is shown in Fig. 3. The sample with the small grains exhibits the lowest mass gain. During oxidation of 44 h a closed, protective Cr_2O_3 layer with an average thickness $d = 1.3 \pm 0.3\,\mu m$ forms, see Fig. 2 g. The surface roughness $R_a \approx 0.3\,\mu m$. Within the Cr_2O_3 layer there are few white particles with a size of around 20 nm, they are identified as W by EDX. Further, there is internal oxidation, formation of localized, disconnected Cr_2O_3 particles inside the metal. On top of the Cr_2O_3 layer, there are a few spots with W-Y-O, potentially also containing a few weight % of Cr. An example is shown in Fig. 2 g. The surface coverage of these oxides is about 4 % in the centre of the sample. At the edge of the sample, within ~ 0.1 mm from the sharp corners, the amount of W-containing oxides is increased.

In contrast, the samples with medium and large grains exhibits a larger mass gain, see Fig. 3. Thus, the sample with large grains forms an oxide layers with a thickness of 8 µm, see Fig. 2 f. On top there is a 0.5 µm thick W-Y-O layer, almost fully covering the 0.3 µm thick Cr_2O_3 layer. Below, there is a thick, porous W-Cr-O layer.

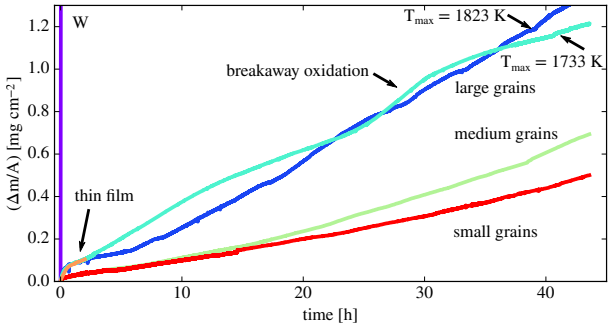

Figure 3: Mass change of a W-11.4Cr-0.6Y alloy and pure W as a function of time. Measurements are preformed at a temperature of 1273 K at 20 kPa O_2 and 80 kPa Ar partial pressure. The samples are produced using different FAST parameters, except for pure W and the thin film which is produced by magnetron sputtering. The corresponding microstructure is shown in Fig. 2

3.2. *Sample preparation*

After optimisation of the grain structure it is important to understand the relevance of the sample surface. For that purpose three samples with the small grains are ground differently:

1. A rough sample is obtained with a surface finish using P180-grade silicon carbide abrasive paper. The surface roughness of the sample $R_a = 0.6\,\mu m$.
2. A round sample is obtained with a surface finish using P1200-grade silicon carbide abrasive paper. The sample is held by hand onto the rotating disc of a planar grinding and polishing machine, very sharp edges are removed. However, a perfectly round shape is not achieved.
3. A standard, cubic sample with a surface finish using P1200-grade silicon carbide abrasive paper. The surface roughness of the sample $R_a = 0.03\,\mu m$.

Fig. 4 shows that the rough sample oxidises almost twice as fast as the round sample which oxidises almost four times faster than the standard, cubic sample.

3.3. *Sublimation measurement and life-time studies*

In section 3.1 it is shown that samples with small grains can maintain the protective oxide layer for at least two days. However, for full passive safety of a future fusion power plant, it is required that the alloy maintains the protective oxide layer for several weeks to suppress sublimation. In this section the results on the oxidation and sublimation performance at 1273 K in synthetic air (20 kPa O_2 and 80 kPa N_2) for weeks of a sample with small grains and a surface finish using P1200-grade silicon carbide abrasive paper are shown. In particular the sublimation measurement, which is performed for the first time, is crucial for qualification of the material.

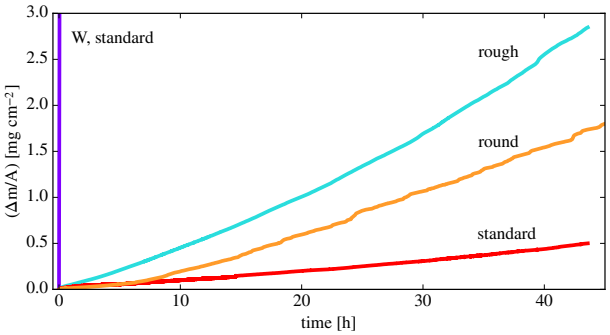

Figure 4: Mass change of a W-11.4Cr-0.6Y alloy and pure W as a function of time. Measurements are preformed at a temperature of 1273 K at 20 kPa O_2 and 80 kPa Ar partial pressure. The surface finish of the alloys is different, else they are identical.

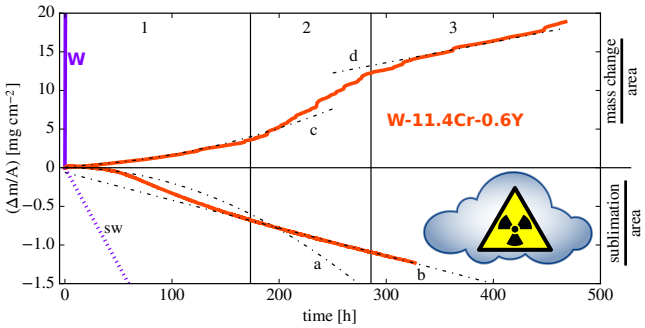

Figure 6: Mass change of a W-11.4Cr-0.6Y alloy and pure W as a function of time. Measurements are preformed in synthetic air at 1273 K. The upper part shows the total mass change of the sample. The lower part, zoomed-in compared to the upper part, shows the sublimation separately. Stages 1-3 and functions a-d are labelled.

The photographs, Fig. 5, show the evolution of the samples. Fig. 5 a shows a ground, cubic samples before oxidation - both the alloy and the pure W samples look that way. Fig. 5 b shows a pure W sample after only 10 h. Volumetric expansion and shape deformation is observed. Fig. 5 c,d show a smart alloy after oxidation for 44 h and 467 h respectively. After 44 h there is slight buckling at the corners of the samples, but overall the initial shape is preserved. After 467 h a porous oxide with blisters is found, but the initial shape can still be clearly recognized.

The corresponding mass change characteristics are shown in Fig. 6. The mass change of the sample is shown in the upper part of the figure, this is the sum of the contribution from sublimation and oxidation. Pure W shows mass gain at a rate of 6×10^{-3} mg cm^{-2} s^{-1}. The mass change of the alloy can be split into three sections: The first section of 180 h shows mass gain with a rate of around 6×10^{-6} mg cm^{-2} s^{-1}. It follows the second section with much faster mass gain of around 2.3×10^{-5} mg cm^{-2} s^{-1} for 100 h. The maximum mass gain rate for a duration of 30 min is 2×10^{-4} mg cm^{-2} s^{-1}. In the third section the mass gain reduces back to around 1.0×10^{-5} mg cm^{-2} s^{-1}.

The bottom part of Fig. 6 shows the contribution from sublimation. The dashed line sw indicates the sublimation rate 7×10^{-6} mg cm^{-2} s^{-1} of pure W. It is measured for the course of 1 h. The solid line shows the sublimation of the alloy. Sublimation is suppressed for about 50 h. In the second and third section of the oxidation process a linear sublimation rate of 1×10^{-6} mg cm^{-2} s^{-1} is observed.

The results of the microstructure analysis after these 467 h of oxidation at 1273 K are shown in Fig. 7. The surface of the sample is shown in Fig. 7 a - W-Cr-O crystals with a size of up to 5 µm and W-Y-O are found. The W-Y-O has a molten-like shape without sharp corners. The full cross section of the oxides, Fig. 7 b, is obtained by embedding the sample in epoxy, removing the first 2 mm from one side, and polishing. At the surface there are W-Cr-Y oxides. Below there follows 20 µm of WO_3 with porosity at the interface to the 31 µm thick Cr_2WO_6 layer. Below the Cr_2WO_6, there is another layer of WO_3 with a thickness of 31 µm before reaching the metal. Internal oxidation of Cr is found within the first 10 µm of the metal. Fig. 7 d shows a magnification of the region labelled (d) in Fig. 7 b. WO_3 and W-16.8Y-18.4O grains with the equivalent spherical diameter of 0.8 µm are seen.

The first few micrometers are damaged after polishing. Therefore, a FIB-cross section, where the surface is protected by a Pt-coating, is also performed - see Fig. 7 c. Different oxides are found: Cr-O, W-Y-O, and W-Cr-O with Cr content in the range of 3 to 12 weight %.

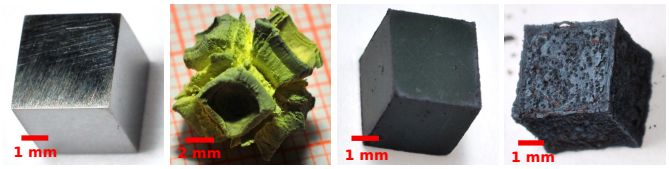

(a) (b) (c) (d)

Figure 5: Photographs of the samples. (a) W-Cr-Y alloy before oxidation after grinding. The pure W samples look the same. (b) Pure W sample after 10 h of oxidation in synthetic air at 1273 K. (c) Optimized W-Cr-Y alloy after 44 h of oxidation in synthetic air at 1273 K. (d) W-Cr-Y alloy after 467 h of oxidation in synthetic air at 1273 K.

4. Discussion

4.1. On FAST optimisation

In section 3.1 it is shown that small grains increase the oxidation resistance, the formation of the protective Cr_2O_3 layer is maintained much longer. The reason is as follows: At 1273 K Cr diffuses mainly along the grain boundaries. Thus, Cr diffusion is faster with smaller grains. Thus, the Cr supply to replenish the protective scale is maintained longer. In the case of larger grains Cr diffusion is slower and Cr depletion below the oxide scale occurs. This yields to the formation of W-containing oxides. They have a large volumetric expansion, break the thin protective Cr_2O_3 layer locally and cause breakaway oxidation. Further, the protective layer can no longer be replenished and the aim, full passive safety, can not be accomplished.

The grain size of the sample is controlled by the FAST production parameters. Grain growth mainly occurs at elevated temperatures, the higher the temperature, the faster is the grain growth. Therefore, the time at elevated temperatures should

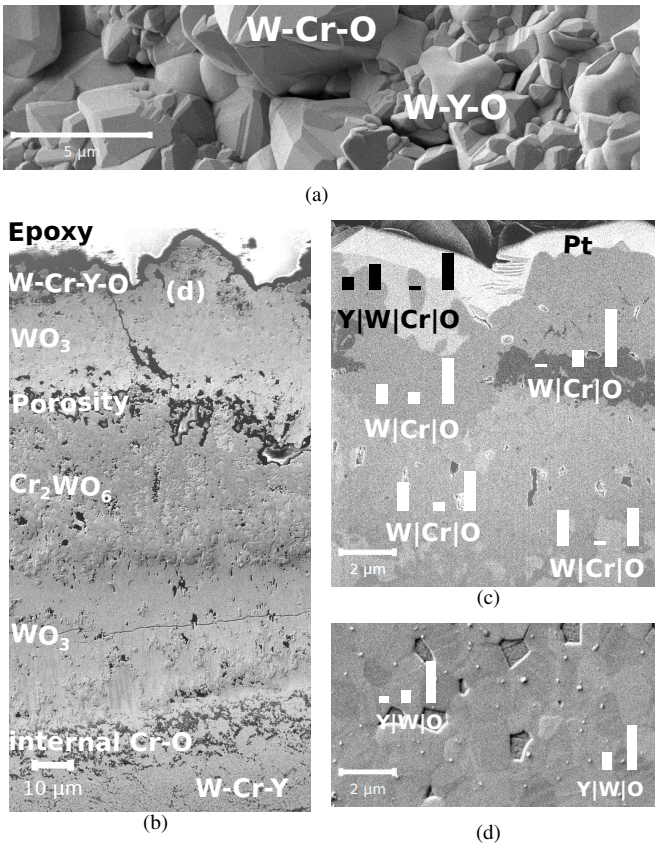

Figure 7: Electon microscopy of the oxide scale after oxidation of an W-11.4Cr-0.6Y alloy for 467 h at 1273 K in synthetic air. The bars on top of the elements indicate the relative atomic composition measured by EDX. The images show the surface view (a) and the cross section of the full oxide scale (b) where the location of image (d) is marked. The cross section shown in (c) is a FIB cut showing the very surface of the sample.

me minimized. This can be achieved by increasing the heating rate h, decreasing the maximum sintering temperature $T_{\max}$, and decreasing the holding time t_{hold}. This rule is confirmed by the results in section 3.1. It is a subject of further research to investigate how much further the grain size can be reduced by reducing the time at elevated temperatures while still achieving good densification.

4.2. On sample preparation

From the cross section in Fig. 3 g it is evident that there are four parameters contributing to the mass gain: mass gain due to formation of the Cr_2O_3 layer, mass gain due to internal oxidation, mass gain due to formation of W-containing oxides, and potentially mass loss due to sublimation. This section requires only a qualitative understanding of these contributions, a quantification is found in section 4.3. If the protective Cr_2O_3 layer fails, the formation of W-containing oxides occurs. Thus W-containing oxide formation is more likely to happen at damages of the surface, such as the edge of the sample.

This explains the observations in Fig. 4: the rough sample has many scratches on the surface. Each scratch is a damage of the surface, increasing the probability for failure of the protective Cr_2O_3. Therefore, more W-containing oxides can form and the mass gain increases compared to the standard sample ground with P1200-grade paper.

The probability of failure of the Cr_2O_3 layer is also increased for the round sample. This is because it is ground hand-held: instead of one defect at the edge of the sample there are many small defects along the rounded surface. Consequently the mass gain is larger compared to the standard sample.

It is expected that a perfectly round sample exhibits a reduced oxidation rate due to the absence of edges which results in less W-containing oxides. This hypothesis can not be verified with the existing grinding methods. However, it could be approached using a larger sample as the fraction of the surface in the vicinity of an edge would decrease.

Another question is, if finer polishing of the sample could yield further improvement of the oxidation resistance. As the surface roughness of the intact oxide layer after 44 h of oxidation is about ten times larger than the initial surface roughness, it is improbable that an even smoother initial surface can yield an improvement of the oxidation resistance.

4.3. On sublimation and life-time studies

In view of the promising results when oxidizing for 2 days, the novel W-Cr-Y alloy with small grains are tested for 3 weeks to approach DEMO-relevant times. The oxidation behaviour shown in Fig. 6 can be understood by estimation of the four contributions to the mass gain Δm_i, $i = 1, 2, 3, 4$:

1. Δm_1 is caused by the formation of the protective Cr_2O_3 layer. This formation is caused by the diffusion of Cr which is described by Fick's first law. Therefore, Δm_1 must follow a parabolic rate law:

$$\Delta m_1/A = \sqrt{c_1 \times t} \tag{1}$$

   where A is the surface area of the sample, t the oxidation time, and c_1 a constant. Using a Cr_2O_3 density of $\rho = 5.2\,\mathrm{g\,cm^{-3}}$, $\Delta m_1/A$ can be transformed to the thickness of the Cr_2O_3 layer. After 44 h the Cr_2O_3 layer is not yet degraded and the thickness is measured at a cross section. With equation 1 this yields $c_1 = 6 \times 10^{-7}\,\mathrm{mg^2\,cm^{-4}\,s^{-1}}$.
2. Δm_2 is caused by the formation of internal Cr_2O_3. This formation is caused by the diffusion of O which is described by Fick's first law. Therefore, Δm_2 must follow a parabolic rate law:

$$\Delta m_2/A = \sqrt{c_2 \times t} \tag{2}$$

   where c_2 is a constant. The area covered by internal oxidation is measured on a cross section after 44 h of oxidation. Knowing the sample dimensions and assuming isotropy of the internal oxide this yields a total volume of internal Cr_2O_3 and thus a mass increase Δm_2. With equation 2 this yields $c_2 = 9 \times 10^{-8}\,\mathrm{mg^2\,cm^{-4}\,s^{-1}}$.
3. Δm_3 is caused by formation of W-containing oxides, typically at spots where the protective oxide layer failed. Failure of the protective oxide and penetration of W through the protective oxide occurs with a certain probability p. Thus, the area covered by W-containing oxides is given by

$$A'(t) = A \times p. \tag{3}$$

At the end of the first oxidation stage, in Fig. 6 after 180 h, the entire sample is effected by failure spots and $A'(t > 180\,\mathrm{h}) = A$

$$\Rightarrow p = \begin{cases} \frac{1}{180\,\mathrm{h}} \times t\,, & t < 180\,\mathrm{h} \\ 1\,, & t > 180\,\mathrm{h} \end{cases} \quad (4)$$

Δm_3 is calculated using this insight and the oxidation rate of mixed oxides c_3:

$$\Delta m_3 = c_3 \times t \times A'(t) \quad (5)$$

4. Δm_4 is the mass loss caused by sublimation of W-containing oxide with the sublimation rate s, the key to asses the improved safety of the power plant:

$$\Delta m_4 = s \times t \times A'(t) \quad (6)$$

Fitting to the data in Fig. 6 yields $s = -1 \times 10^{-6}\,\mathrm{mg\,cm^{-2}\,s^{-1}}$ from function b and $c_3 = 6 \times 10^{-6}\,\mathrm{mg\,cm^{-2}\,s^{-1}}$ from function c. Functions a and d are calculated according to the model described above. For function d an additional offset of $5\,\mathrm{mg\,cm^{-2}}$ is required as the second section of the oxidation process is not described by this model. The hypothesis is that there builds up a slight Cr depletion under the protective oxide layer during the first section. This accelerates the oxidation in the second section.

The goal of suppression of sublimation to avoid radioactive contamination of the environment in case of a LOCA is achieved according to equation 6. This means that there is very little release within the first two days. Later, sublimation with the rate s is found. For a reactor with a first wall surface of $1000\,\mathrm{m^2}$ this implies a potential release of 21 kg with an activity of 1×10^{16} Bq per month. These numbers apply for dry air, in humid air the release could be 10 to 100 times higher [14]. However, even in dry air, this is a severe hazard for the environment, in comparison the total release due to the nuclear accident in Fukushima was 6×10^{17} Bq [15]. However, it should be remarked that one could solve the problem with smart alloys if the cooling was switched back on. With pure W this would not be possible as the first wall would be mechanically destructed as one can imagine from the photograph shown in Fig. 5 b.

The oxidation time in the experiment presented in Fig. 7, is sufficiently long to form oxides according to the phase diagram [16]. That implies that in the presence of W-containing oxides the initially formed Cr_2O_3 layer degrades into WO_3 and Cr_2WO_6. The Y does not form a stoichiometric oxide with the W, instead it approaches W-14Y-20.8O, which should only form in a molten phase starting from 1427 K. According to the phase diagram [17], this is the solution with the lowest melting point. Thus, the sample is at around 90 % of the melting point of that phase during the experiment. Therefore, the W-Y-O on the surface of the sample, Fig. 7 a has a molten-like shape. In order to suppress the sublimation, future developments should attempt to suppress the formation of this compound.

5. Conclusion and Outlook

W is a promising candidate as plasma facing armour material for future fusion power plants. Oxidation and sublimation is a major problem in case of air ingress in a LOCA. W-Cr-Y alloys are suggested to avoid a complete mechanical destruction of the first wall and to avoid radioactive contamination of the environment. It is found that the sintering should be optimized towards small grains. Further, it is crucial to have a smooth surface. With a grain size of 0.1 to 0.2 µm and a roughness $R_a = 0.03\,\mu\mathrm{m}$ the formation of a protective Cr_2O_3 layer and suppression of sublimation for two days at 1273 K is shown. After that significant sublimation of radioactive W-oxides is measured and it would be required to restart cooling. Complete mechanical destruction can be avoided successfully, but the goal of full passive safety is not achieved yet. Therefore, the development of advanced W-alloys must continue. One option for further optimisation is to attempt to reduce the grain size further. Another option is to investigate other or additional active elements, such as Zr, to further support the formation of a protective Cr_2O_3 layer.

6. Acknowledgements

A part of this work has been carried out within the framework of the EUROfusion Consortium and has received funding from the Euratom research and training programme 2014 - 2018 under grant agreement No 633053. The views and opinions expressed herein do not necessarily reflect those of the European Commission.

References

[1] J. W. Coenen, S. Antusch, M. Aumann, et al. Materials for demo and reactor applicationsboundary conditions and new concepts. *Phys. Scr.*, 2016(T167):014002, 2016.

[2] Y. Ueda, K. Schmid, M. Balden, et al. Baseline high heat flux and plasma facing materials for fusion. *Nucl. Fusion*, 57(9):092006, 2017.

[3] Ch. Linsmeier et al. Development of advanced high heat flux and plasma-facing materials. *Nucl. Fusion*, 57(9):092007, 2017.

[4] M. R. Gilbert, J.-C. Sublet, and R. A. Forrest. *Handbook of activation, transmutation, and radiation damage properties of the elements simulated using FISPACT-II & TENDL.* Culham Center For Fusion Energy, 2015.

[5] D. Maisonnier, I. Cook, et al. The european power plant conceptual study. *Fusion Eng. Des.*, (75-79):1173–1179, 2005.

[6] T. Wegener, F. Klein, A. Litnovsky, et al. Development and analyses of self-passivating tungsten alloys for demo accidental conditions. *Fusion Eng. Des.*, https://doi.org/10.1016/j.fusengdes.2017.03.072, 2017.

[7] J. R. Davis, editor. *ASM Specialty Handbook: Heat-Resistant Materials*. S. D. Henry, 1999.

[8] T. Wegener, F. Klein, A. Litnovsky, et al. Development of yttrium-containing self-passivating tungsten alloys for future fusion power plant. *Nuclear Materials and Energy*, 9:394–398, 2016.

[9] A. Litnovsky, T. Wegener, F. Klein, et al. New oxidation-resistant tungsten alloys for use in the nuclear fusion reactors. *Phys. Scr.*, T170(014012), 2017.

[10] A. Litnovsky, T. Wegener, F. Klein, et al. Advanced smart tungsten alloys for a future fusion power plant. *Plasma Phys. Control. Fusion*, 59:064003, 2017.

[11] O. Guillon, J. Gonzalez-Julian, B. Dargatz, et al. Field-assisted sintering technology / spark plasma sintering: Mechanisms, materials, and technology developments. *Adv. Eng. Mater.*, 16(7):830–849, 2014.

[12] A. Calvo, C. Garcia-Rosales, F. Koch, et al. Manufacturing and testing of self-passivating tungsten alloys of different composition. *Nuclear Materials and Energy*, 9:422–429, 2016.

[13] S. Telu, R. Mitra, and S. Kumar Pabi. Effect of Y_2O_3 addition on oxidation behavior of W-Cr alloys. *Metallurgical and Materials Transactions A*, 46(12):5909–5919, 2015.

[14] A. Litnovsky, F. Klein, T. Wegener, et al. Smart first wall materials for intrinsic safety of a future power plant. In *ISFNT-13, Kyoto, Japan, 25 Sep 2017 - 29 Sep 2017*, 2017.

[15] G. Steinhauser, A. Brandl, and T. E. Johnson. Comparison of the chernobyl and fukushima nuclear accidents: A review of the environmental impacts. *Science of The Total Environment*, 470 - 471:800 – 817, 2014.

[16] K. T. Jacob. Phase relationships in the system Cr-W-O and thermodynamic properties of $CrWO_4$ and Cr_2WO_6. *J. Mater. Sci.*, 15(9):2167–2174, 1980.

[17] H. J. Borchardt. Yttrium-tungsten oxides. *Inorg Chem*, 2(1):170–173, 1963.